

Nanoporous alumina formation in a thin magnetron-sputtered Al layer

Konstantinas Leinartas*,

Povilas Miečinskas,

Algirdas Selskis,

Eimutis Juzeliūnas

*Institute of Chemistry,
Goštauto 9,
LT-01108 Vilnius,
Lithuania*

The magnetron sputtering technique was used for thin Al layer formation on Si wafers. The parameters of the sputtering process were experimentally estimated. The substrate temperature range of 9–12 °C was determined as most favorable for the deposition of uniform Al coatings. Thin, porous alumina layers with pore diameters close to 10–15 nm were formed by galvanostatic oxidation of sputtered coatings in an oxalic acid solution. A porous layer thickness of 40–60 nm was evaluated as close to that minimally needed for the further surface finishing.

Key words: nanoporous alumina, thin layers, anodizing, magnetron sputtering, scanning electron microscopy

INTRODUCTION

Conversion of solar energy to electricity is one of the most urgent scientific and technical problems. Most of today's solar cells (SC), assigned to the first generation, are based on crystalline silicon and till now remain one of the most promising patterns. The highest yield of planar monocrystall silicon SC with one *p-n* junction is 25% which is close to the thermodynamic limit of ~30% [1]. A promising strategy for improving the efficiency of SCs is to orthogonize light absorption and charge separation directions. The structuring of SC surface by formation of nanodimensional wires, columns or pores would allow to achieve the mentioned aims.

In recent years, intensive studies of processes enabling to compose nanostructured metal or semiconducting formations on Si surface have been carried out. One of the promising processes used for the formation of ordered structures is the so-called spontaneous electrochemical self-assembly of porous alumina while anodizing pure metallic Al [2–4]. Under certain conditions, the anodic oxidation of aluminum in mineral or organic acids leads to formation of a porous hydrated oxide layer: a tidy structure (matrix), which consists of densely packed hexagonal columnar cells with cylinder pores in the center. A schematic view of such a porous alumina layer is presented in Fig. 1.

During electrolysis, nodi of pores are formed at the oxide / electrolyte interface, and they develop perpendicular to the substrate surface [5]. There are several theories explaining the initiation of pores and their self-assembly in the oxide Al layer during anodizing. One of the first mechanisms of pore formation was proposed by Sullivan and Wood [6]. They further developed Hoar and Mott's concept of field-assisted dissolution [7]. According to this theory, during Al anodizing, a strong external electric field "stretches" and breaks the Al–O bonds in the superficial layer of the Al oxide / solution interface. Therefore, metal dissolution is facilitated and the emerged lattice vacancies become the potential centers of

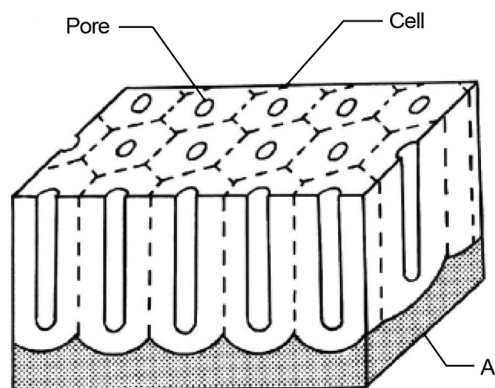


Fig. 1. Scheme of porous alumina layer structure [2]

* Corresponding author. E-mail: leinart@ktl.mii.lt

pore formation. The electric field also promotes the growth of the porous layer, i. e. due to an increasing curvature of pores, the corresponding enhancement of the imposed electric field accelerates Al^{3+} emission into solution (Fig. 2). On the other hand, the barrier layer (compact alumina), which is formed at the pore walls and bottoms, brakes the growth of the oxide layer. Both competing processes – field-assisted dissolution and barrier layer formation – determine the overall kinetics of porous layer formation. Sullivan and Wood's model was experimentally approved by many other authors.

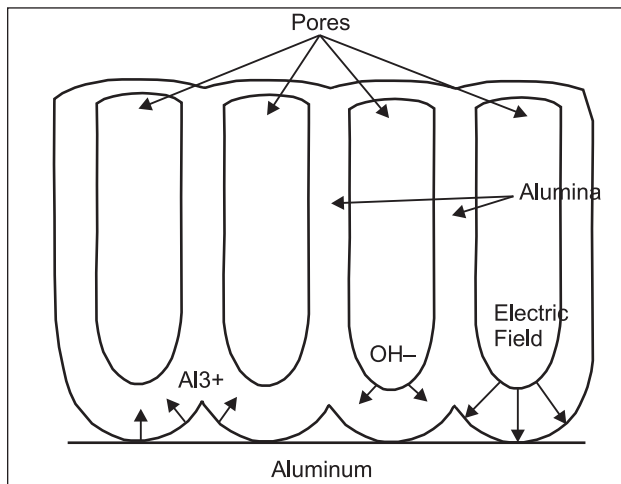


Fig. 2. A scheme of “field-assisted” formation of alumina porous layer [8]

An alternative model of pore formation and layer growth was proposed by Shimuzu et al. [9]. According to this mechanism, new pores are formed due to tensile stresses in the oxide layer when the “barrier-type” growth transforms into the “porous-type” one. It is known that these oxide types are characterized by different Pilling–Bedworth ratios. Due to the difference in the molar volume of the above oxides, large local tensions in the layer emerge and cause cracks in the “weak” areas. Usually, the “weak” areas are surface micro-defects (ridges, microcracks), lattice defects, dislocations, etc. The emerged micro / nanocracks are ‘healed’ while anodizing, but the oxide layer over these areas is much thinner. The formed oxide surface is uneven, and the locally thinner areas are preferential for pore initiation.

The structure of the porous layer (diameter and distance between the pores) was determined to depend on anodizing conditions (the acid nature and solution pH, temperature, anodizing voltage (U) or current density (i) and nature (purity) of the substrate) [8, 10–13]. A porous layer of the preferential structure is formed when 25–30% of Al in the form of Al^{3+} passes into solution. These conditions are realized best in phosphorus, oxalic, sulfuric and chromic acids. The properties of a porous alumina layer are highly dependent on electrolyte temperature: more compact and hard layers are formed in solutions at a temperature 0–20 °C as compared to those formed at higher temperatures (>60 °C). The dissolution rate

of Al at higher temperatures of acids is increased, and a substantially thinner and less hard oxide layer is formed [14].

The problems of the pore self-assembly mechanism during anodizing, pore formation and porous layer growth are equally important. According to Jessensky [15], mechanical tensions generated in a growing oxide layer cause the repulsive forces between the neighboring pores. The interaction between tension and repulsive forces induces the pores’ self-regulation and self-assembly. On the basis of the alumina layer empirical porosity degree ~ 1.4 (volume expansion of the aluminum during oxidation) in phosphorus, oxalic and sulfuric acids, it was calculated that the corresponding compression forces should be equivalent to 4 GPa [16]. The essential influence of inward mechanical stresses during film growth on the generation of pores was emphasized by Skeldon et al. [17]. The above tensions originate from both film material (aluminum and oxygen ions) and solution ions’ displacement from the barrier layer towards the cell walls. The shape of the barrier surface, the power of the imposed electric field, field-assisted ionic losses of the layer material to the electrolyte and the plasticity of the aluminum oxide may be interlinked and related to the external anodizing parameters.

The diameter of the formed pores (d) varied from a few to several hundred nanometers, and the depth might reach several microns. By anodizing over 100 μm , thick porous layers can be formed. Empirical dependences of pore diameter and the distance between them (L) on the electrolysis voltage were determined [18, 19]:

$$d \approx (1.29 \text{ nm/V}) \times U \quad (1)$$

$$L \approx (2.5 \text{ nm/V}) \times U. \quad (2)$$

Empirical dependence (2) is quite accurate in the voltage range $U = 10\text{--}50$ V, but a relatively large deviation was determined over the range limits. The values of L significantly depend on electrolyte temperature and anodizing duration. Predictions according to formula (1) are less accurate. As is mentioned, the d values greatly depend on the nature of acid and oxide exposure time to the electrolyte.

Most works on porous layer formation were performed with relatively thick (several mm) bulk Al coatings. The anodizing of thin layers (<1 μm) is much less studied. From the practical point of view, it is also important to note that porous layer formation is usually only an “intermediate” stage in the sequence of Si surface nanostructuring procedures. For this reason, the thickness of the porous layer minimally needed for further finishing procedures (chemical or / and physical) is a point of significant interest. Also, it can be mentioned that the present work is the initial stage of works on the nanostructuring of Si surface with p–n junction.

The goals of the study were: a) to form smooth thin porous alumina layers by anodic oxidation of magnetron-sputtered Al and b) to evaluate the thickness of the formed porous layer minimally needed for further nanostructuring procedures.

EXPERIMENTAL

Thin Al layers on Si wafers (20×20 mm) were deposited using a UNIVEX 350 magnetron-sputtering device (Leybold, Germany). This device is equipped with three confocal ST-20 magnetrons (AJA International) and can operate both in DC (direct current) and RF (radio frequency) modes. Targets were prepared from highly pure Al (99.999%, Alfa Aesar GmbH). The anodizing of magnetron-deposited Al coatings was carried out in an electrochemical cell in a 0.3 M oxalic acid solution (pure *p. a.* CHEMPUR, Poland) at a temperature of 20 °C with an Agilent 6038 power supply source (USA). A special holder was designed to support coated silicon wafers (Fig. 3). This arrangement prevents from an undesirable touch of the back (also covered with Al for test purposes) Si surface and electrical contacts with the acidic anodizing solution. The working electrode (a circle of Al-coated Si wafer exposed to solution) area was 2 cm². A platinum plate (20×25 mm) was used as an auxiliary electrode.

After porous alumina layer formation, the rest of the barrier layer at the bottom of pores was removed by chemical etching in 5 wt.% orthophosphoric acid solutions.

The composition of magnetron-sputtered coatings, the distribution of nanopores in Al oxide layers and Au nanocolumns on the Si surface were determined with an EVO-50-XVP scanning electron microscope (SEM) (Carl Zeiss SMT AG, Germany). The thickness of coatings was evaluated with a Dektak 6M profilometer (VEECO, USA).

RESULTS AND DISCUSSION

The first stage of the current study consisted of an empirical determination of the optimal sputtering parameters allowing deposition of thin amorphous (nanostructured) uniform Al

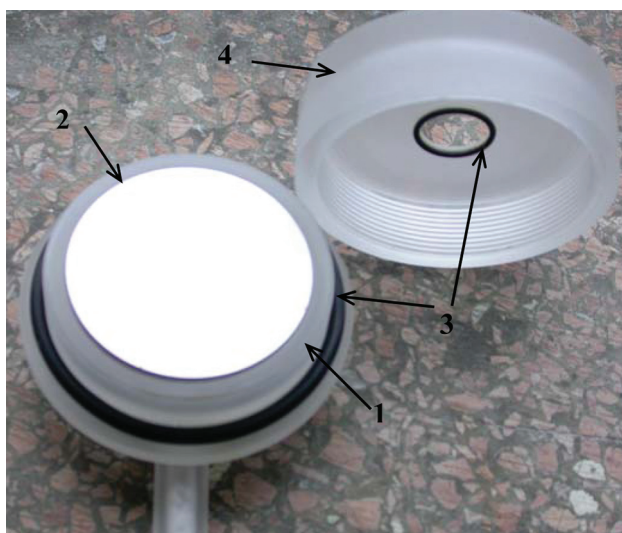


Fig. 3. The holder used for anodizing thin Al layers sputtered on Si wafers. 1 – main “body” of holder, 2 – Si wafer (disc) covered with sputtered Al, 3 – rub-bish rings, 4 – holder’s sealant cap

layers on Si wafers. Before sputtering, the UNIVEX 350 device chamber was vacuumated to $(1.2\text{--}1.6) \times 10^{-6}$ mBar. After the chamber vacuumation was completed, it was filled with the operation gas (Ar), and the Si wafer surface (substrate) was cleaned with Ar⁺ ions in RF mode. The RF plasma discharge was maintained at a pressure of 6.5×10^{-3} mBar and 16 W of effective power for 5 minutes. Magnetron sputtering of the Al target was carried out in DC mode: the working gas pressure

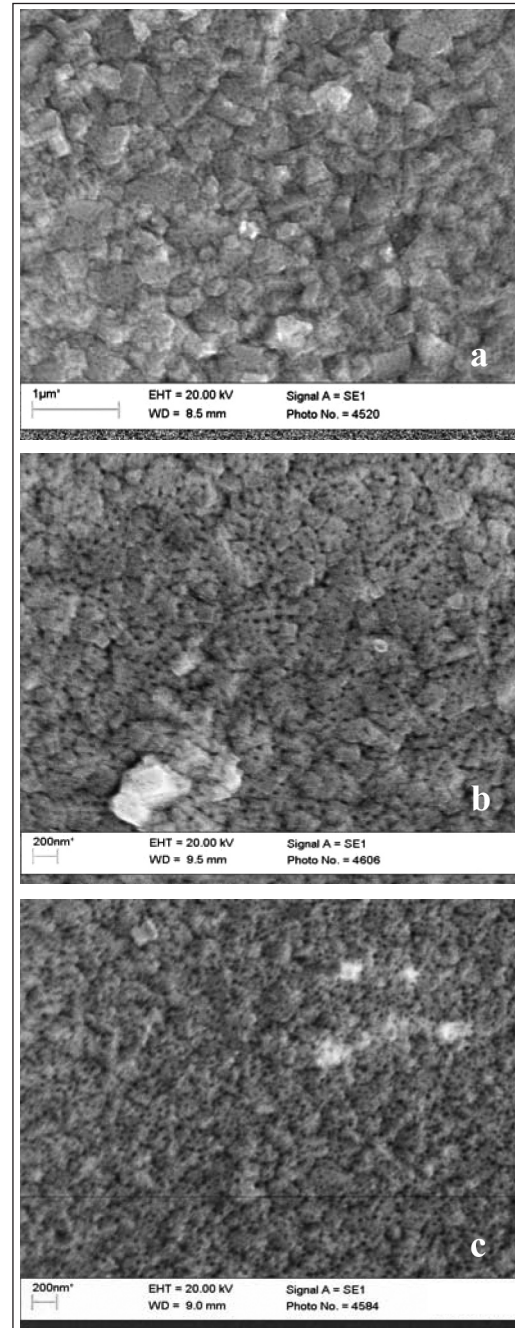


Fig. 4. SEM images of Al surfaces sputtered at 80 (a), 60 (b), 40 °C (c). *a* – Al coating potentiostatically anodized at 40 V for 4 min, *b* – Al coatings galvanostatically anodized at 4 mA/cm² (pore-developing voltage 44 V, duration 3 min) and *c* – Al coatings galvanostatically anodized at 3 mA/cm² (pore-developing voltage 43.5 V, duration 6 min)

was $\sim 1.3 \times 10^{-3}$ mbar and the power of sputtering was maintained at ~ 270 W. Though a high-quality Al coatings were deposited at a wide temperature range, it was determined that the ones best suitable for further amorphous porous layer formation were deposited at 9–12 °C of the substrate. Coatings deposited at higher temperatures were not smooth, and this was an essential impediment to achieve an ordered pore distribution during the further anodizing. SEM images of the surface of Al coatings formed at 80, 60 and 40 °C and routinely anodized are shown in Fig. 4. As one can see, large-scale aggregates are characteristic of the morphology of the surfaces, and though pores were formed on the aggregate plates and edges, the distribution of the former over the surface was not uniform.

As was experimentally determined, sputtering duration for the deposition of 100–500 nm thick Al coatings was 10–25 min. For the best distribution of the Al layer thickness over the Si surface, the substrate was rotated at 13 rpm, and the distance between the target and substrate was about ~ 15 cm. A typical thickness distribution of sputtered Al coating on Si wafer in respect to the disc center is shown in Fig. 5 (curve 1). At the edges of coatings, its thickness discrepancy was -14% to $+24\%$ in respect to the average one (the symbol “minus” means less thickness). It is obvious that layer thickness deviations at the edges of the wafers were determined by the construction of the sputtering device (as three confocal magnetrons in the chamber are situated at an angle to the substrate). The thickness nonuniformity of Al deposits was reduced to -5% and $+7\%$ when the shield of the operational DC magnetron had been modified so that more of sputtered Al would reach the substrate (Fig. 5, curve 2).

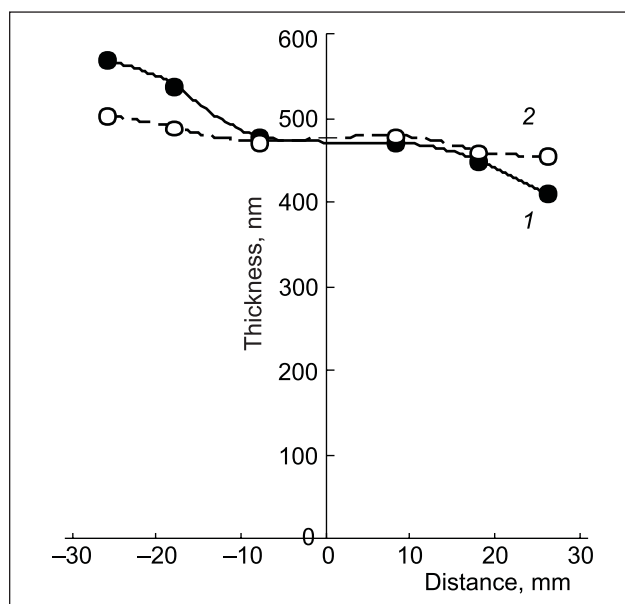


Fig. 5. Distribution of sputtered Al layer thickness over the Si disc: 1 – Al coating deposited with a standard magnetron shield, 2 – Al coating deposited with a modified magnetron shield

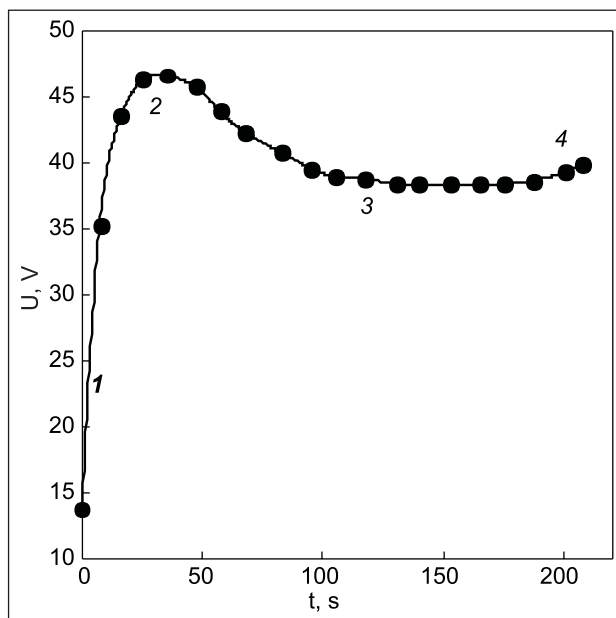


Fig. 6. Voltage dependence on anodizing time (4 mA cm^{-2})

Also, 5–15 W power RF etching of the substrates was imposed simultaneously with DC sputtering, but no essential influence on the thickness distribution and pore diameters was determined.

Both potentiostatic and galvanostatic methods were used for anodizing sputtered Al coatings. The best patterns of alumina nanoporous layers were formed by the galvanostatic anodizing method. The anodizing procedures were performed in an oxalic acid solution with the commonly used electrochemical equipment. Si wafers coated with a thin Al layer were mounted in a special holder (Fig. 3) and placed in an electrochemical vessel filled with an oxalic acid electrolyte. To avoid spontaneous dissolution of Al in the acidic solution, the working anodizing power had been applied to the sample before it was placed in the working vessel. A typical voltage dependence on the anodizing time of a thin Al layer on the Si substrate is shown in Fig. 6. As one can see, the measured dependence had four characteristic parts attributed to the following processes: 1) barrier layer formation, 2) pore formation, 3) development (growth) of pores and 4) beginning of Si substrate oxidation. The power source (current) was turned off when Si dissolution began.

After electrochemical oxidation, alumina that remained at the bottom of pores was removed (chemically etched) in a 5 wt.% orthophosphoric acid solution. This procedure was performed in a separate vessel after the Si wafer sample had been dismantled from the anodizing holder. The volume of the pickling solution was about 200 ml, the solution temperature was 30 °C. The solution was stirred with a magnetic stirrer during sample etching. The etching time varied from 7 to 30 min.

The composition of sputtered layers was controlled; the shape, distribution and size of alumina pores were evaluated

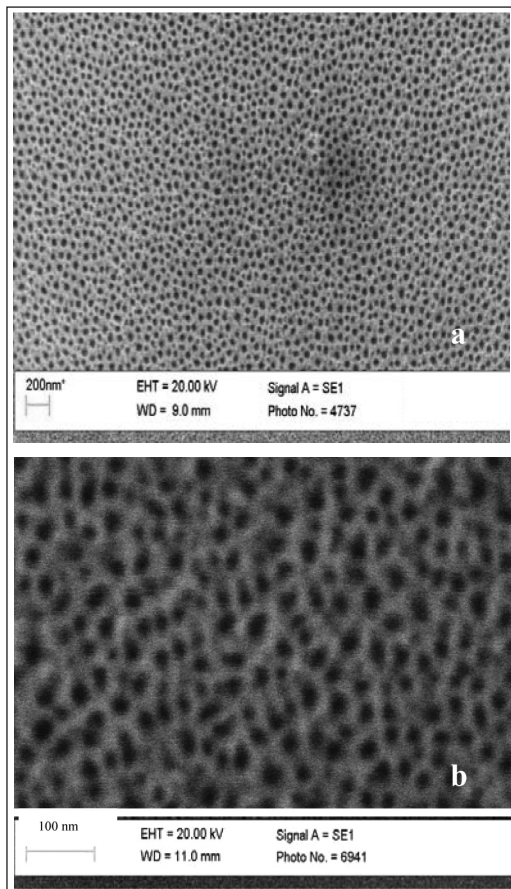


Fig. 7. *a* – SEM image of porous alumina surface formed by anodizing a magnetron-sputtered Al coating in oxalic acid (current 4 mA/cm², voltage 46 V, time 75 s) and 15 min etching in orthophosphoric acid solution; *b* – SEM image of a porous alumina surface formed by anodizing a magnetron-sputtered Al coating in oxalic acid (current 4 mA/cm², voltage 18 V, time 60 s) and 9 min etching in orthophosphoric acid solution

by SEM. SEM images of the surface of porous layers formed in magnetron-sputtered Al coatings after anodizing in oxalic acid and chemical etching in H₃PO₄ solution are presented in Fig. 7. The anodizing and etching conditions of sputtered layers are given in figure captions. For the porous layer presented in Fig. 7a SEM image, the pore diameter ranged from ~20 to ~45 nm and of the layer in Fig. 7b from ~10–15 to ~25–30 nm. For both patterns, the anodizing current was 4 mA/cm². As is generally known, the diameter of pores and the distance between them mainly depend on the anodizing voltage (equations 1 and 2). The pore-developing voltage was 46 V in the former case, and in the latter case it was essentially lower – 18 V. During anodizing and chemical etching procedures, alongside with pore formation, coating dissolution (reduction) occurs. For example, the initial thickness of the sputtered Al coating presented in Fig. 7a was about 180 nm. After the above procedures, the overall thickness of the porous Al oxide layer on the Si wafer was about 60 nm. The coating thickness decreased by about 100–120 nm during chemical etching in orthophosphoric acid. Preliminary

studies on the chemical deposition of metal nanocolumns in pores have shown that the 40–50 nm thickness of the porous layer is enough for the needed structure formation. A notable phenomenon was determined in the etching of porous Al layers in orthophosphoric acid: the pore diameter was slightly influenced by the duration of the above stage, although this operation is often used for widening bulk (thick) Al pores.

CONCLUSIONS

1. The parameters of the magnetron-sputtering process of the formation of thin (100–500 nm) nanostructured Al layers on Si substrates were experimentally determined. The temperature range 9–12 °C of the substrate was evaluated as most favorable for the deposition of uniform nanostructured Al coatings.

2. Pores about 10–15 nm in diameter were formed by the galvanostatic anodizing of sputtered Al layers in oxalic acid.

3. A porous layer thickness of 40–60 nm was evaluated as close to that minimally needed for the further surface finishing.

ACKNOWLEDGEMENT

The project was supported by the Lithuanian State Science and Studies Foundation (Contract No. B-39/2009).

Received 22 September 2009

Accepted 6 October 2009

References

1. W. Shockley, H. J. Queissier, *J. Appl. Phys.*, **32**, 510 (1961).
2. H. Masuda, F. Hasegawa, S. Ono, *J. Electrochem. Soc.*, **144**, L276 (1997).
3. S. Ono, M. Saito, H. Asoh, *Electrochim. Acta*, **51**, 827 (2005).
4. Z. Chu, K. Wada, S. Inoue, M. Isogai, K. Katsuta, A. Yashumuri, *J. Electrochem. Soc.*, **153**, B384 (2006).
5. F. Keller, M. S. Hunter, D. L. Robinson, *J. Electrochem. Soc.*, **100**, 411 (1953).
6. J. O'Sullivan, G. Wood, *Proc. Roy. Soc. Lon.*, **A317**, 511 (1970).
7. T. Hoar, N. Mott, *J. Phys. Chem. Solids*, **9**, 957 (1959).
8. K. Wada, T. Shimohira, M. Yamada, N. Baba, *J. Electrochem. Soc.*, **22**, 3810 (1986).
9. K. Shimuzu, K. Kobayashi, G. Tompson, G. Wood, *Phil. Mag. A*, **6**, 643 (1992).
10. G. Thomson, G. Wood, in: J. Scully (ed.), *Treatise on Material Science Technology*. **23. Corrosion: Aqueous Processes and Passive Films**, Academic Press, NY (1983), p. 205–329.
11. V. P. Parkhutik, J. M. Albella, Y. E. Makushok, I. Montero, J. Martinex-Duart, V. I. Shershulskii, *Electrochim. Acta*, **35**, 955 (1990).

12. S. Ono, H. Ichinose, T. Kawaguchi, N. Masuka, *Surf. Sci.*, **31**, 249 (1990).
13. J. A. Treverton, J. Ball, D. Johnson, J. C. Vickerman, R. H. West, *Surf. Interface Anal.*, **16**, 369 (1990).
14. J. Diggle, T. Downie, C. Goulding, *Chem. Rev.*, **69**, 365 (1969).
15. O. Jessensky, F. Muller, U. Goele, *Appl. Phys. Lett.*, **72**, 1173 (1998).
16. A.-P. Li, F. Muller, A. Birner, K. Nielsch, U. Goele, *J. Appl. Phys.*, **84**, 6023 (1998).
17. S. J. Garcia-Vergara, L. Iglesias-Rubianes, C. E. Blanco-Pinzon, P. Skeldon, G. E. Thompson, P. Campestrini, *Proc. Royal Soc. A*, **462**, 2345 (2006).
18. J. O'Sullivan, G. Wood, *Proc. Roy. Soc. A*, **317**, 511 (1970).
19. M. M. Crouse, A. E. Miller, D. T. Crouse, A. A. Ikramb, *J. Electrochem. Soc.*, **152**, D167 (2005).

Konstantinas Leinartas, Povilas Miečinskas, Algirdas Selskis,
Eimutis Juzeliūnas

NANOPORINGO ALIUMINIO OKSIDO FORMAVIMAS AL DANGOJE, NUSODINTOJE MAGNETRONINIO DULKINIMO METODU

S a n t r a u k a

Ploni Al sluoksniai buvo formuoti ant Si plokštelių pastovios srovės magnetroninio dulkinimo metodu. Empiriškai įvertinti optimalūs dangų nusodinimo parametrai. Nustatyta, kad substrato temperatūrų diapazonas 9–12 °C yra palankiausias tolygioms Al dangoms formuoti. Ploni, porėti aliuminio oksido sluoksniai, kuriuose porų skersmuo apie 10–15 nm, buvo suformuoti oksalo rūgšties tirpale galvanostatinio anodavimo metodu. Nustatyta, kad tolesnėms paviršiaus nanostruktūravimo procedūroms atlikti pakanka 40–60 nm storio poringos Al dangos.